Contemporary Mathematics
https://ojs.wiserpub.com/index.php/CM/

Research Article

Dynamical Systems Perspective on a Stochastic SIR Model with Multiplicative Noise

Shah Hussain[1*], Mohammed Alghazi[2†], Najla A. Mohammed[3], Ilyas Khan[2,4,5]

[1] Department of Mathematics, College of Science, University of Hail, Hail, 2440, Saudi Arabia
[2] Department of Mathematics, College of Science Al-Zulfi, Majmaah University, Al-Majmaah, 11952, Saudi Arabia
[3] Mathematics Department, Faculty of Sciences, Umm Al-Qura University, Makkah, Saudi Arabia
[4] Department of Mathematical Sciences, Saveetha School of Engineering, SIMATS, Chennai, Tamil Nadu, India
[5] Applied Science Research Center. Applied Science Private University, Amman, Jordan
E-mail: s.khan@uoh.edu.sa; M.alghizzi@mu.edu.sa

Received: 29 October 2025; **Revised:** 21 November 2025; **Accepted:** 12 December 2025

Abstract: We analyze a stochastic Susceptible-Infected-Recovered (SIR) epidemic model incorporating multiplicative environmental noise. Starting from positive initial conditions, we establish global existence, uniqueness, and strict positivity of strong solutions. Using the Lyapunov function method, we derive time-average fluctuation bounds around the disease-free equilibrium when $R_0 < 1$ and around the endemic equilibrium when $R_0 > 1$. In the stochastic setting, a noise-adjusted reproduction number is obtained via a logarithmic transformation of the infected population, $\tilde{R}_0 = \dfrac{\beta(\Lambda/d)}{d+\gamma+\frac{1}{2}\sigma_2^2}$, which explicitly reduces to the deterministic basic reproduction number $R_0 = \dfrac{\beta\Lambda}{d(d+\gamma)}$ when $\sigma_2 = 0$, ensuring consistency with Section 6. Under this threshold, the infection becomes extinct almost surely if $\tilde{R}_0 < 1$, while additional analytical results establish stochastic persistence when $\tilde{R}_0 > 1$. Numerical simulations employing the Milstein scheme confirm these analytical findings: increasing the noise intensity σ_2 amplifies fluctuations and can shift long-run behavior from persistence to extinction. Extensions to include additional removal terms $h(I)$ are briefly discussed.

***Keywords*:** Susceptible-Infected-Recovered (SIR) model, basic reproduction number, stochastic differential equations, numerical simulations

MSC: 92D30, 92B05, 34D20

1. Introduction

Understanding how environmental variability shapes epidemic dynamics has motivated extensive work on stochastic epidemic models. While deterministic Susceptible-Infected-Recovered (SIR) frameworks provide a sharp threshold criteria in terms of the basic reproduction number R_0 [1–3], real-world transmission is subject to random fluctuations (behavioral shifts, climate, reporting noise) that can qualitatively alter long-run behavior [4–6]. This paper revisits the classical SIR model under multiplicative noise and establishes extinction and persistence conditions that remain informative beyond the deterministic setting.

DOI: https://doi.org/10.37256/cm.7120269024

In the deterministic SIR model with recruitment rate Λ, natural removal rate d, recovery rate γ, and transmission rate β, the Disease-Free Equilibrium (DFE) $\left(\frac{\Lambda}{d},\, 0,\, 0\right)$ is globally attractive when

$$R_0 \;=\; \frac{\beta(\Lambda/d)}{d+\gamma} \;<\; 1,$$

whereas an endemic equilibrium exists for $R_0 > 1$ [1–3]. Introducing multiplicative noise into the infection dynamics modifies this picture: the logarithmic Itô equation for the infected compartment contributes an additional drift term $-\frac{1}{2}\sigma_2^2$ from quadratic variation [7]. A natural noise-adjusted threshold therefore emerges,

$$\widetilde{R}_0 = \frac{\beta(\Lambda/d)}{d+\gamma+\frac{1}{2}\sigma_2^2}. \tag{1}$$

under which infection goes extinct almost surely when $\tilde{R}_0 < 1$, while complementary Lyapunov bounds support stochastic persistence when $\tilde{R}_0 > 1$ [8–11]. This contrast highlights how environmental variability can effectively "tax" transmission and shift the persistence boundary relative to the deterministic R_0.

Stochastic Susceptible-Infected-Susceptible (SIS)/SIR-type models have been analyzed via martingale and Lyapunov techniques to obtain positivity, moment bounds, extinction criteria, and stationary distributions [12]. In particular, log-transform arguments for infected dynamics together with Foster-Lyapunov functions for permanence are now standard analytical tools [6, 7]. Our analysis follows this thread while focusing on quantities with direct epidemiological meaning (extinction a.s. vs. persistence in mean) and on transparency of assumptions and constants; numerically, we employ Milstein discretization for strong approximations [13].

The novelty here is twofold: (i) a transparent log-I derivation of the noise-adjusted threshold (5) that cleanly separates extinction from persistence in small-to-moderate noise regimes; and (ii) a quadratic Lyapunov framework that yields explicit time-average bounds around both the DFE and the endemic regime. Compared with prior results emphasizing stationary measures or asymptotic moments [6, 10], we provide conditions that are interpretable and directly actionable for model calibration and simulation design. We also outline how the framework extends to additional removal terms $h(I)$, indicating where the threshold and Lyapunov bounds would need to be adapted [11].

In summary, we prove global existence, uniqueness, and strict positivity of solutions for the stochastic SIR model with multiplicative noise [6, 7]; derive an extinction condition $\tilde{R}_0 < 1$ from the log-I equation, and establish complementary persistence-in-mean bounds for $\tilde{R}_0 > 1$ [9–11]; and provide reproducible numerical experiments (Milstein scheme) illustrating extinction/persistence transitions as σ_2 varies [6, 13].

Structure of the paper: Section 2 introduces the stochastic SIR model, notation, and assumptions (independent Brownian motions; local Lipschitz and linear growth). Section 3 establishes global existence, strict positivity, and moment bounds. Fluctuation bounds near the disease-free equilibrium ($R_0 < 1$) appear in Section 4, while Section 5 treats the endemic equilibrium ($R_0 > 1$) via a quadratic Lyapunov approach. Section 6 derives the extinction threshold $\tilde{R}_0$ and the complementary persistence-in-mean result. Section 7 reports Milstein simulations illustrating the transition from persistence to extinction as σ_2 increases, and Section 8 concludes.

2. Model formulation

We consider a stochastic SIR model with multiplicative noise on each compartment. Let $X(t) = (S(t),\, I(t),\, R(t))^\top$ denote the state and $\{B_i(t)\}_{i=1}^3$ be independent standard Brownian motions on a filtered probability space satisfying the usual conditions. The use of Stochastic Differential Equations (SDEs) for epidemic dynamics with recent extensions

(media effects, vaccination, awareness, and delay/network structures) is well documented in the modern literature [14–17]. The dynamics are

$$\mathrm{d}S(t) = \big(\Lambda - \beta S(t)I(t) - dS(t)\big)\,\mathrm{d}t \;+\; \sigma_1 S(t)\,\mathrm{d}B_1(t), \tag{2}$$

$$\mathrm{d}I(t) = \big(\beta S(t)I(t) - (d+\gamma)I(t)\big)\,\mathrm{d}t \;+\; \sigma_2 I(t)\,\mathrm{d}B_2(t), \tag{3}$$

$$\mathrm{d}R(t) = \big(\gamma I(t) - R(t)\big)\,\mathrm{d}t \;+\; \sigma_3 R(t)\,\mathrm{d}B_3(t), \tag{4}$$

with parameters $\Lambda,\ \beta,\ \gamma,\ d > 0$ and noise intensities $\sigma_1,\ \sigma_2,\ \sigma_3 \geq 0$. The multiplicative structure and parameterization align with recent stochastic SIR/Susceptible-Infected-Recovered-Susceptible (SIRS) generalizations (including Lévy/white-noise perturbations) [18, 19]. Initial data are taken in the positive orthant $\mathbb{R}^3_+$ with $S(0),\ I(0),\ R(0) > 0$.

The multiplicative form reflects proportional fluctuations within each compartment: (i) σ_1 captures variability in recruitment and effective contact affecting susceptibles (seasonality, behavioral shifts, reporting noise); (ii) σ_2 modulates the infection/removal pressure on infectives (contact heterogeneity, interventions, environmental drivers); (iii) σ_3 captures variability in recovery/waning or reporting of removed individuals. Dimensional check: since $\mathrm{d}B_i$ has units $t^{1/2}$, each σ_i has units $t^{-1/2}$, so $\frac{1}{2}\sigma_i^2$ has units of a rate. While we assume independent sources $B_1,\ B_2,\ B_3$, correlated environmental shocks can be modeled via non-diagonal diffusion (e.g., correlated Brownian motions) [20].

Unless stated otherwise, $B_1,\ B_2$ and B_3 are mutually independent. (Correlated noise can be handled by replacing the diagonal diffusion with a full covariance structure and adapting the Lyapunov analysis; see [20] for a recent construction with vaccination).

Define the drift $b(x) = \big(\Lambda - \beta si - ds,\ \beta si - (d+\gamma)i,\ \gamma i - dr\big)$ and diffusion matrix $\Sigma(x) = \mathrm{diag}(\sigma_1 s,\ \sigma_2 i,\ \sigma_3 r)$. Here $b(x) = (f_1(x),\ f_2(x),\ f_3(x))^\top$ and $\Sigma(x) = \mathrm{diag}(g_1(x),\ g_2(x),\ g_3(x))$, where $x = (S,\ I,\ R)^\top$. On $\mathbb{R}^3_+$, b and Σ are locally Lipschitz and satisfy a linear-growth bound

$$\|b(x)\| + \|\Sigma(x)\| \leq K\,(1 + \|x\|) \quad \text{for some } K > 0,$$

so by standard SDE theory there exists a unique global strong solution for positive initial data; recent SDE epidemic works verify existence, uniqueness, strict positivity, and threshold behavior under closely related assumptions [21]. Moreover, the boundary of the positive orthant is inaccessible under (2)-(4), hence solutions remain strictly positive a.s. We note that these formulations are compatible with modern network/extended-compartment settings [22, 23] and with contemporary threshold/identifiability viewpoints using effective reproduction numbers in stochastic environments [24, 25].

We consistently use: β (transmission rate), γ (recovery rate), d (natural removal rate), Λ (recruitment), and $(\sigma_1,\ \sigma_2,\ \sigma_3)$ (noise intensities).

The deterministic basic reproduction number follows from the next-generation matrix $F = \beta S$, $V = d + \gamma$ giving $R_0 = \dfrac{F}{V} = \dfrac{\beta\Lambda}{d(d+\gamma)}$ and the noise adjusted threshold employed later is

$$\tilde{R}_0 \;=\; \frac{\beta\,(\Lambda/d)}{d + \gamma + \dfrac{1}{2}\sigma_2^2}, \tag{5}$$

as derived in Section 6 (see Theorem 6.2 and the definition in (5)).

3. Global existence and positivity

We work on a complete filtered probability space $(\Omega,\ \mathscr{F},\ (\mathscr{F}_t)_{t\geq 0},\ P)$ supporting three independent standard Brownian motions $B_1,\ B_2,\ B_3$. Parameters satisfy $\Lambda,\ \beta,\ \gamma,\ d > 0$ and noise intensities $\sigma_i \geq 0$. Initial data are $(S(0),\ I(0),\ R(0)) \in (0,\ \infty) \times (0,\ \infty) \times [0,\ \infty)$ and are $\mathscr{F}_0$-measurable.

Theorem 3.1 (Global well-posedness and strict positivity) The stochastic SIR system (2) admits a unique strong solution $(S(t),\ I(t),\ R(t))_{t\geq 0}$ defined for all almost surely. Moreover,

$$S(t) > 0, \quad I(t) > 0, \quad R(t) > 0 \quad \text{for all } t > 0 \text{ a.s.} \tag{6}$$

Proof. Step 1 (Local existence and pathwise uniqueness): [26] The drift and diffusion coefficients are polynomials (hence C^∞) on $\mathbb{R}^3$. On every bounded set, they are globally Lipschitz. Therefore the system satisfies the standard local Lipschitz and linear growth on compacts conditions, ensuring a unique strong solution up to an explosion time $\tau_e \in (0,\ \infty]$.

Step 2 (Non-explosion: $\tau_e = \infty$ a.s.): We assume strictly positive initial conditions $S(0) > 0$ and $I(0) > 0$, ensuring positivity of the solution.

We define the total population process as

$$N(t) := S(t) + I(t) + R(t), \tag{7}$$

which satisfies the stochastic differential equation

$$dN(t) = (\Lambda - dN(t))\,dt + \sigma_1 S(t)\,dB_1(t) + \sigma_2 I(t)\,dB_2(t) + \sigma_3 R(t)\,dB_3(t). \tag{8}$$

For $k \in \mathbb{N}$, define $\tau_k := \inf\{t \geq 0 : N(t) \geq k\}$. On $[0,\ \tau_k]$ we have $0 \leq S,\ I,\ R \leq k$. Taking expectations and applying Gronwall-type estimates yields boundedness of $\mathbb{E}N(t \wedge \tau_k)$ (the operator $\mathbb{E}$ denotes mathematical expectation), which implies $P(\tau_k \leq t) \to 0$ as $k \to \infty$. Hence $\tau_e = \infty$ a.s.

Step 3 (Strict positivity):

(a) Infectious class. Using Itô's formula on $\ln I(t)$ and a stopping argument, one obtains

$$I(t) = I(0) \exp\left\{ \int_0^t \left(\beta S(s) - (d+\gamma) - \frac{1}{2}\sigma_2^2 \right) ds + \sigma_2 B_2(t) \right\} > 0 \quad \text{a.s.} \tag{9}$$

(b) Susceptible class. The S-equation can be solved explicitly as

$$S(t) = \Phi_1(t) \left(S(0) + \int_0^t \Phi_1(s)^{-1} \Lambda\, ds \right), \tag{10}$$

$$\Phi_1(t) := \exp\left\{ \int_0^t \left(-\beta I(s) - d - \frac{1}{2}\sigma_1^2 \right) ds + \sigma_1 B_1(t) \right\} > 0, \tag{11}$$

so $S(t) > 0$.

(c) Recovered class. Similarly,

$$R(t) = \Phi_3(t)\left(R(0) + \int_0^t \Phi_3(s)^{-1}\gamma I(s)\,ds\right), \tag{12}$$

$$\Phi_3(t) := \exp\left\{\int_0^t \left(-d - \frac{1}{2}\sigma_3^2\right)ds + \sigma_3 B_3(t)\right\} > 0. \tag{13}$$

With $I(s) > 0$ and $R(0) \geq 0$, this gives $R(t) > 0$.
Thus, each compartment remains strictly positive for all $t > 0$.
Remark 3.2 (Moment bounds) The estimate in Step 2 implies

$$\sup_{t\geq 0} \mathbb{E}N(t) \leq N(0) + \Lambda/d, \tag{14}$$

and similar bounds hold for higher moments by applying Itô to N^p. These are later used to control time averages.

4. Fluctuations near the disease-free equilibrium ($R_0 < 1$)

We recall that the disease-free equilibrium is given by

$$S_o = \frac{\Lambda}{d}, \qquad I_o = 0, \qquad R_o = 0. \tag{15}$$

Let $x := S - S_o$, $i := I$, $r := R$, where $S_o = \Lambda/d$ denotes the susceptible level at the disease-free equilibrium. We study fluctuations around the DFE $E_0 = (S_o,\ 0,\ 0)$ using a quadratic Lyapunov function that includes a cross term to neutralize the drift coupling between x and i.

4.1 *Lyapunov function and generator calculation*

Consider

$$V(x,\ i,\ r) = x^2 + \kappa i^2 + \rho r^2 + \delta\, x\, i, \tag{16}$$

with $\delta = 2$, the mixed drift term $\propto Sxi$ cancels exactly in the generator verified from Section 2,

$$dx = (-\beta Si - dx)\,dt + \sigma_1 S\,dB_1, \tag{17}$$

$$di = (\beta Si - (d+\gamma)i)\,dt + \sigma_2 i\,dB_2, \tag{18}$$

$$dr = (\gamma i - dr)\,dt + \sigma_3 r\,dB_3, \tag{19}$$

where $S = x + S_o$ and $B_1,\ B_2,\ B_3$ are independent Brownian motions.

Lemma 4.1 (Generator identity) The infinitesimal generator $\mathscr{L}$ applied to V satisfies

$$\begin{aligned} LV = &(-2dx^2 + \sigma_1^2 S^2) + \left(2\kappa\beta S - 2\kappa(d+\gamma) + \kappa\sigma_2^2\right) i^2 \\ &+ \left(2\rho\gamma ri - 2\rho d r^2 + \rho\sigma_3^2 r^2\right) \\ &+ \left(2\beta S xi - 2(d+\gamma)xi - 2\beta S i^2 - 2dxi\right). \end{aligned} \tag{20}$$

Proof. Apply Itô's formula to each term: $(dx)^2 = \sigma_1^2 S^2\,dt$, $(di)^2 = \sigma_2^2 i^2\,dt$, $(dr)^2 = \sigma_3^2 r^2\,dt$, and $d\langle x,i\rangle = d\langle x,\ r\rangle = d\langle i,\ r\rangle = 0$ because the Brownian motions are independent. Collecting drifts, the terms $-2\beta Sxi$ (from x^2) and $+2\beta Sxi$ (from δxi) cancel as $\delta = 2$. □

4.2 *A priori bounds near the DFE*

We control the remaining mixed terms using Young's inequalities and the identity $S^2 = (x+S_o)^2 \le 2x^2 + 2S_o^2$.

Lemma 4.2 (Quadratic bound) For any $\varepsilon > 0$ and any $\eta > 0$,

$$\begin{aligned} LV \ \le\ &-\left(d - 2\sigma_1^2 - \varepsilon\right)x^2 \\ &+\left(2\kappa\beta S - 2\kappa(d+\gamma) + \kappa\sigma_2^2 + \frac{(\rho\gamma^2)}{d} + \frac{(2(2d+\gamma))^2}{\eta}\right) i^2, \\ &-\rho\left(d - \sigma_3^2\right) r^2 + 2\sigma_1^2 {S_o}^2 + \varepsilon x^2 + \eta x^2. \end{aligned}$$

Proof. Use $\sigma_1^2 S^2 \le 2\sigma_1^2 x^2 + 2\sigma_1^2 S_o^2$. For couplings, apply Young: $2\rho\gamma ri \le \rho d r^2 + \dfrac{(\rho\gamma^2)}{d} i^2$ and $|-2(2d+\gamma)xi| \le \eta x^2 + (2(2d+\gamma))^2 i^2/\eta$. Group terms to obtain the bound. □

To remove the remaining S in the i^2 coefficient uniformly, observe that $\kappa \in (0,\ 1)$ implies $2\kappa\beta S - 2\beta S = 2\beta S(\kappa - 1) \le 0$; discarding this nonpositive contribution yields a uniform upper bound.

Corollary 4.3 (Uniform coercive bound) Assume

$$\sigma_1^2 < \frac{d}{2}, \quad \sigma_3^2 < d. \tag{21}$$

Pick $\varepsilon,\ \eta > 0$ such that $\alpha_1 := d - 2\sigma_1^2 - \varepsilon - \eta > 0$. Select $\kappa \in (0,\ 1)$ and $\rho \in \left(0,\ \dfrac{d-\sigma_3^2}{d}\right]$ so that

$$\alpha_2 := 2\kappa(d+\gamma) - \kappa\sigma_2^2 - \frac{\rho\gamma^2}{d} - \frac{(2(2d+\gamma))^2}{\eta} > 0, \tag{22}$$

$$\alpha_3 := \rho(d - \sigma_3^2) > 0. \tag{23}$$

Then, for all $(x,\ i,\ r)$,

$$\mathscr{L}V \le -\alpha_1 x^2 - \alpha_2 i^2 - \alpha_3 r^2 + C_0, \quad C_0 := 2\sigma_1^2 S_o^2. \tag{24}$$

Proof. Combine Lemma 4.2 with $2\beta S(\kappa-1)i^2 \le 0$. □

4.3 *Time-average fluctuation bound around the DFE*

Let $\tau_M := \inf\{t \ge 0 : \max(S(t),\ I(t),\ R(t)) \ge M\}$ for $M \in \mathbb{N}$.

Theorem 4.4 (Time-average quadratic bound near the DFE) Assume $R_0 < 1$ and under the parameter conditions in Corollary 4.3, all coefficients satisfy $\alpha_1 > 0$, $\alpha_2 > 0$, and $\alpha_3 > 0$, hence the denominator below uses $\min\{\alpha_1,\ \alpha_2,\ \alpha_3\} > 0$. Then for every positive initial condition,

$$\limsup_{t\to\infty} \frac{1}{t}\mathbb{E}\int_0^t \left(x(s)^2 + i(s)^2 + r(s)^2\right) ds \le \frac{C_0 + V(0)}{\min\{\alpha_1,\ \alpha_2,\ \alpha_3\}}. \tag{25}$$

Proof. Apply Itô's formula to $V(x(t\wedge\tau_M),\ i(t\wedge\tau_M),\ r(t\wedge\tau_M))$. The local martingale has zero mean, hence

$$\mathbb{E}V(t\wedge\tau_M) = \mathbb{E}V(0) + \mathbb{E}\int_0^{t\wedge\tau_M} (\mathscr{L}V)(s)\, ds.$$

Using Corollary 4.3,

$$\mathbb{E}V(t\wedge\tau_M) + \alpha\,\mathbb{E}\int_0^{t\wedge\tau_M} \left(x^2 + i^2 + r^2\right) ds \le \mathbb{E}V(0) + C_0 t, \quad \alpha = \min\{\alpha_1,\ \alpha_2,\ \alpha_3\}.$$

Divide by t and let $t \to \infty$, then let $M \to \infty$. By Theorem 3.1, $\tau_M \to \infty$ a.s.; Fatou's lemma yields the claim. □

Remark 4.5 (Interpretation) The constants α_j describe a small-noise regime where the drift is near E_0 dominates diffusion. Choosing $\kappa \in (0,1)$ ensures the S-dependent contribution to i^2 is nonpositive, taming transmission-induced fluctuations. The constant term C_0 arises from noise in the susceptible equation and scales with σ_1^2 and $S_o = \Lambda/d$. Background on Lyapunov methods and stopped processes can be found in [12].

5. Fluctuations near the endemic equilibrium ($R_0 > 1$)

Assume $R_0 = \beta\Lambda/[d(d+\gamma)] > 1$. The deterministic system admits an endemic equilibrium $E_o = (S_o,\ I_o,\ R_o)$ given by

$$S_o = \frac{d+\gamma}{\beta}, \tag{26}$$

$$I_o = \frac{\Lambda}{d} - S_o, \tag{27}$$

$$R_o = \frac{\gamma}{d} I_o. \tag{28}$$

Set deviations $u := S - S_o$, $v := I - I_o$, and $w := R - R_o$. We derive a time-average bound around E^* under small-noise conditions, ensuring that stabilizing drift dominates stochastic perturbations near E^*.

5.1 *Linearization and Lyapunov candidate*

Assume $R_0 = \beta\Lambda/[d(d+\gamma)] > 1$. The deterministic system admits the endemic equilibrium

$$(S_o,\, I_o,\, R_o) = \left(\frac{d+\gamma}{\beta},\, \frac{\Lambda}{d} - \frac{d+\gamma}{\beta},\, \frac{\gamma}{d}\left(\frac{\Lambda}{d} - \frac{d+\gamma}{\beta} \right) \right).$$

Introduce deviations $u := S - S_o$, $v := I - I_o$, $w := R - R_o$. Substitution of $S = u + S_o$, $I = v + I_o$, $R = w + R_o$ into (2)-(4) gives the linearized drift and multiplicative noise terms

$$du = (-(\beta I_o + d)\, u - \beta S_o v - \beta uv)\, dt + \sigma_1 (u + S_o)\, dB_1,$$

$$dv = (\beta I_o u + (\beta S_o - (d+\gamma))v + \beta uv)\, dt + \sigma_2 (v + I_o)\, dB_2,$$

$$dw = (\gamma v - dw)\, dt + \sigma_3 (w + R_o)\, dB_3.$$

To study stability, consider the quadratic Lyapunov function

$$W(u,\, v,\, w) = a u^2 + b v^2 + c w^2 + 2quv, \qquad a,\, b,\, c > 0,\, ab - q^2 > 0.$$

To eliminate the cross-interaction in the linearized drift, select

$$q := -\frac{\beta I_o + d}{2}, \tag{29}$$

This choice avoids the dimensional inconsistency in $\beta(S_o - I_o)$ because $S_o,\, I_o$ represent population sizes, whereas β has units of inverse population per time. The expression above follows from the Jacobian condition $\beta S_o = d + \gamma$ at the endemic equilibrium.

Applying Itô's formula yield

$$LW \le -\alpha_u u^2 - \alpha_v v^2 - \alpha_w w^2 + K_0 + K_1 |uv|,$$

where $u,\, v,\, w$ are scalar quantities, hence the mixed term must appear as $K_1|uv|$ rather than $K_1 uv$.

Using Young's inequality,

$$K_1|uv| \le \eta u^2 + \frac{K_1^2}{4\eta} v^2, \qquad \forall \eta > 0,$$

where the squared factor K_1^2 is essential.

Selecting $\eta > 0$ sufficiently small and diffusion intensities $\sigma_1,\ \sigma_2,\ \sigma_3$ sufficiently small ensures that

$$\tilde{\alpha}_u := \alpha_u - \eta > 0, \qquad \tilde{\alpha}_v := \alpha_v - \frac{K_1^2}{4\eta} > 0, \qquad \tilde{\alpha}_w := \alpha_w > 0,$$

so the Lyapunov drift becomes strictly negative outside a bounded region, establishing a coercive quadratic Lyapunov estimator near the endemic equilibrium.

5.2 *Generator estimate*

By Itô's formula and independence of $B_1,\ B_2,\ B_3$, the diffusion part adds $a\sigma_1^2(u+S_o)^2$, $b\sigma_2^2(v+I_o)^2$, $c\sigma_3^2(w+R_o)^2$. For the drift (ignoring βuv momentarily), the quadratic terms form

$$\begin{aligned} \mathscr{L}_0 W = &-2a(\beta I_o + d)u^2 + 2b(\beta S_o - (d+\gamma))v^2 - 2cdw^2 \\ &+ 2q\left(\beta I_o u^2 - (\beta I_o + d)uv + (\beta S_o - (d+\gamma))uv - \beta S_o v^2\right). \end{aligned} \tag{30}$$

Choose q to cancel the linearized uv term:

$$q = \frac{\beta S_o - (d+\gamma) - (\beta I_o + d)}{2} = \frac{\beta(S_o - I_o) - (2d+\gamma)}{2}. \tag{31}$$

The remaining cubic term βuv will be controlled by Young's inequality.

Incorporating diffusion and using $(u+S_o)^2 \le 2u^2 + 2S_o^2$ (and analogs for $v,\ w$), we get

$$\mathscr{L}W \le -\alpha_u u^2 - \alpha_v v^2 - \alpha_w w^2 + K_0 + K_1|uv|, \tag{32}$$

with

$$\alpha_u = 2a(\beta I_o + d) - 2a\sigma_1^2 - |2q|(\beta I_o + d), \tag{33}$$

$$\alpha_v = 2\left(b((d+\gamma) - \beta S_o) + q\beta S_o\right) - 2b\sigma_2^2, \tag{34}$$

$$\alpha_w = 2cd - 2c\sigma_3^2, \tag{35}$$

and

$$K_0 = 2a\sigma_1^2 S_o^2 + 2b\sigma_2^2 I_o^2 + 2c\sigma_3^2 R_o^2, \tag{36}$$

$$K_1 = \beta(b + |q|). \tag{37}$$

Applying Young's inequality to $|uv|$, for any $\eta > 0$:

$$K_1|uv| \leq \eta u^2 + \frac{K_1^2}{4\eta} v^2. \tag{38}$$

Choosing η small and $a,\ b,\ c > 0$ so that

$$\tilde{\alpha}_u := \alpha_u - \eta > 0, \tag{39}$$

$$\tilde{\alpha}_v := \alpha_v - \frac{K_1^2}{4\eta} > 0, \tag{40}$$

$$\tilde{\alpha}_w := \alpha_w > 0, \tag{41}$$

yields the coercive generator bound

$$\mathscr{L}W \leq -\tilde{\alpha}_u u^2 - \tilde{\alpha}_v v^2 - \tilde{\alpha}_w w^2 + K_0, \tag{42}$$

valid for a small-noise regime near E^*.

5.3 *Time-average fluctuation bound near the endemic equilibrium*

Let $\tau_M := \inf\{t \geq 0 : \max(|u(t)|,\ |v(t)|,\ |w(t)|) \geq M\}$.

Theorem 5.1 (Time-average quadratic bound near the Endemic Equilibrium (EE)) Suppose $R_0 > 1$ and pick $a,\ b,\ c > 0$, $q \in \mathbb{R}$, and $\eta > 0$ so that $\tilde{\alpha}_u,\ \tilde{\alpha}_v,\ \tilde{\alpha}_w > 0$. Then for every positive initial condition,

$$\limsup_{t\to\infty} \frac{1}{t}\,\mathbb{E}\int_0^t \left(u(s)^2 + v(s)^2 + w(s)^2\right) ds \leq \frac{K_0 + \mathbb{E}W(0)}{\min\{\tilde{\alpha}_u,\ \tilde{\alpha}_v,\ \tilde{\alpha}_w\}}. \tag{43}$$

Proof. Apply Itô's formula to $W(u(t\wedge\tau_M),\ v(t\wedge\tau_M),\ w(t\wedge\tau_M))$. The local martingale has zero mean, hence

$$\mathbb{E}W(t\wedge\tau_M) = \mathbb{E}W(0) + \mathbb{E}\int_0^{t\wedge\tau_M} (\mathscr{L}W)(s)\, ds.$$

Use the coercive bound and proceed as in Theorem 4.4 to conclude:

$$\mathbb{E}W(t\wedge\tau_M)+\tilde{\alpha}\,\mathbb{E}\int_0^{t\wedge\tau_M}\left(u^2+v^2+w^2\right)ds\le \mathbb{E}W(0)+K_0t,\quad \tilde{\alpha}=\min\{\tilde{\alpha}_u,\ \tilde{\alpha}_v,\ \tilde{\alpha}_w\}.$$

Divide by t and let $t\to\infty$; then send $M\to\infty$. Non-explosion (Theorem 3.1) implies $\tau_M\to\infty$ a.s.; Fatou's lemma yields the result. □

Remark 5.2 (Choice of parameters) A convenient selection is $a=b=c=1$ with q as chosen above; then choose η small and require σ_i small enough so that $\tilde{\alpha}_u,\ \tilde{\alpha}_v,\ \tilde{\alpha}_w>0$. This reflects a standard small-diffusion regime: the deterministic linear drift stabilizes $(u,\ v,\ w)$ around E^*, while diffusion contributes only a bounded forcing term proportional to K_0.

6. Extinction and the stochastic reproduction number

To characterize extinction under environmental noise, we introduce the noise-adjusted reproduction number obtained from the logarithmic drift of the infected class. Applying Itô's formula to $\ln I(t)$ yields a modified threshold in the presence of multiplicative noise. Accordingly, we define

$$\tilde{R}_0=\frac{\beta(\Lambda/d)}{d+\gamma+\frac{1}{2}\sigma_2^2}. \tag{44}$$

This expression is consistent with the deterministic basic reproduction number $R_0=\dfrac{\beta\Lambda}{d(d+\gamma)}$ and reduces exactly to R_0 when the noise intensity $\sigma_2=0$. Thus, $\tilde{R}_0$ provides a stochastic generalization of the classical threshold.

Remark 6.1 The boundary case $\tilde{R}_0=1$ corresponds to a critical regime where higher-order terms determine dynamics. In this case, fluctuations may drive the infection to extinction with probability one, and the deterministic equilibrium loses stability.

Theorem 6.2 (Extinction criterion) If $\tilde{R}_0<1$, then for any positive initial condition,

$$\lim_{t\to\infty} I(t)=0\quad\text{almost surely.} \tag{45}$$

Proof. We proceed in four transparent steps, using standard stopping, martingale Strong Law of Large Numbers (SLLN), and time-average identities.

Let $N:=S+I+R$. For $M\in\mathbb{N}$, define the stopping time

$$\tau_M:=\inf\{t\ge 0:\max(S(t),\ I(t),\ R(t))\ge M\}. \tag{46}$$

By Theorem 3.1 (global existence; non-explosion), $\tau_M\uparrow\infty$ a.s. as $M\to\infty$.

We will work on $[0,\ t\wedge\tau_M]$, where all processes are bounded by M. This guarantees that all local martingales appearing below have quadratic variation $\langle\cdot\rangle(t)=O(t)$, hence their time averages vanish a.s. by the martingale strong law of large numbers.

For any process X, write the stopped time-average

$$\overline{X}_{t,\,M} := \frac{1}{t}\int_0^{t\wedge\tau_M} X(s)\,ds. \tag{47}$$

(2a) For $N = S+I+R$. Summing the SDEs gives

$$dN(t) = (\Lambda - dN(t))\,dt + \sigma_1 S\,dB_1 + \sigma_2 I\,dB_2 + \sigma_3 R\,dB_3. \tag{48}$$

Here, $B_1(t)$, $B_2(t)$, and $B_3(t)$ are independent standard Brownian motions. Thus, the noise term $\sigma_1 S\,dB_1 + \sigma_2 I\,dB_2 + \sigma_3 R\,dB_3$ has no cross-covariation terms.

Integrate on $[0,\ t\wedge\tau_M]$, divide by t, and rearrange:

$$\overline{N}_{t,\,M} = \frac{\Lambda}{d} - \frac{N(t\wedge\tau_M)-N(0)}{dt} - \frac{M_N(t)}{dt}, \tag{49}$$

where $M_N(t) := \int_0^{t\wedge\tau_M}(\sigma_1 S\,dB_1 + \sigma_2 I\,dB_2 + \sigma_3 R\,dB_3)$. Since $|N(t\wedge\tau_M)| \le 3M$ and $\langle M_N\rangle(t) = \int_0^{t\wedge\tau_M}(\sigma_1^2 S^2 + \sigma_2^2 I^2 + \sigma_3^2 R^2)\,ds \le Ct$,

$$\frac{N(t\wedge\tau_M)-N(0)}{t} \to 0, \quad \frac{M_N(t)}{t} \to 0 \quad \text{a.s.},$$

hence

$$\overline{N}_{t,\,M} \xrightarrow[t\to\infty]{} \Lambda/d \quad \text{a.s.} \tag{50}$$

(2b) For R vs I. From $dR = \gamma I\,dt - dR\,dt + \sigma_3 R\,dB_3$,

$$\overline{I}_{t,\,M} = \frac{d}{\gamma}\overline{R}_{t,\,M} + \frac{R(t\wedge\tau_M)-R(0)}{\gamma t} - \frac{M_R(t)}{\gamma t}, \tag{51}$$

with $M_R(t) := \int_0^{t\wedge\tau_M}\sigma_3 R\,dB_3$. The boundary term and $M_R(t)/t$ vanish a.s., so

$$\overline{R}_{t,\,M} = \frac{\gamma}{d}\overline{I}_{t,\,M} + o(1) \quad \text{a.s.} \tag{52}$$

(2c) For S. Since $S = N - I - R$,

$$\overline{S}_{t,\,M} = \overline{N}_{t,\,M} - \overline{I}_{t,\,M} - \overline{R}_{t,\,M}$$

$$= \frac{\Lambda}{d} - \left(1+\frac{\gamma}{d}\right)\overline{I}_{t,\,M} + o(1) \quad \text{a.s.} \tag{53}$$

That is,

$$\overline{S}_{t,\,M} = \frac{\Lambda}{d} - \left(1+\frac{\gamma}{d}\right)\overline{I}_{t,\,M} + o(1) \quad \text{a.s.} \tag{54}$$

Indeed, since $S = N - I - R$, taking stopped time averages gives $\overline{S}_{t,\,M} = \overline{N}_{t,\,M} - \overline{I}_{t,\,M} - \overline{R}_{t,\,M}$. Using $\overline{N}_{t,\,M} \to \Lambda/d$ from (50) and $\overline{R}_{t,\,M} = \dfrac{\gamma}{d}\overline{I}_{t,\,M} + o(1)$ from (52), we obtain

$$\overline{S}_{t,\,M} = \frac{\Lambda}{d} - \left(1+\frac{\gamma}{d}\right)\overline{I}_{t,\,M} + o(1),$$

which confirms the algebraic identity.

By Itô's formula for $\ln I$ (valid since $I > 0$ a.s. by Theorem 3.1), on $[0,\, t \wedge \tau_M]$,

$$\ln I(t\wedge\tau_M) = \ln I(0) + \int_0^{t\wedge\tau_M} \left(\beta S(s) - (d+\gamma) - \frac{1}{2}\sigma_2^2\right) ds + \sigma_2 B_2(t\wedge\tau_M). \tag{55}$$

Note that Itô's formula for $\ln I(t)$ is valid only when $I(t) > 0$. By Theorem 3.1, the solution of the SDE satisfies $I(t) > 0$ for all $t \geq 0$ almost surely, hence the application above is justified.

Divide by t:

$$\frac{\ln I(t\wedge\tau_M)}{t} = \frac{\ln I(0)}{t} + \beta\overline{S}_{t,\,M} - (d+\gamma) - \frac{1}{2}\sigma_2^2 + \sigma_2\frac{B_2(t\wedge\tau_M)}{t}. \tag{56}$$

Moreover, the term $\sigma_2 B_2(t\wedge\tau_M)/t$ converges to 0 a.s. This follows from the strong law of large numbers for martingales, since $B_2(t\wedge\tau_M)$ is a martingale with quadratic variation of order $O(t)$.

The Brownian term satisfies $B_2(t\wedge\tau_M)/t \to 0$ a.s. (quadratic variation $\leq Ct$). Using (54) for $\overline{S}_{t,\,M}$,

$$\frac{\ln I(t\wedge\tau_M)}{t} = c_0 - \beta\left(1+\frac{\gamma}{d}\right)\overline{I}_{t,\,M} + o(1) + \sigma_2\frac{B_2(t\wedge\tau_M)}{t} + \frac{\ln I(0)}{t}, \tag{57}$$

where

$$c_0 := \beta\frac{\Lambda}{d} - (d+\gamma) - \frac{1}{2}\sigma_2^2 > 0 \quad (\text{since } \tilde{R}_0 > 1). \tag{58}$$

The condition $c_0 > 0$ is equivalent to

$$\beta\frac{\Lambda}{d} - (d+\gamma) - \frac{1}{2}\sigma_2^2 > 0 \quad \Longleftrightarrow \quad \tilde{R}_0 > 1,$$

making the persistence threshold explicit.

Rearrange:

$$\beta\left(1+\frac{\gamma}{d}\right)\bar{I}_{t,\,M} = c_0 + o(1) + \sigma_2 \frac{B_2(t\wedge\tau_M)}{t} - \frac{\ln I(t\wedge\tau_M)}{t} + \frac{\ln I(0)}{t}. \tag{59}$$

Because $0 < I(t\wedge\tau_M) \le M$, we have $\ln I(t\wedge\tau_M) \le \ln M$.
Since $0 < I(t\wedge\tau_M) \le M$, we have $\ln I(t\wedge\tau_M) \le \ln M$. Dividing by t gives

$$\frac{\ln I(t\wedge\tau_M)}{t} \le \frac{\ln M}{t}.$$

Taking lim sup on both sides yields

$$\limsup_{t\to\infty} \frac{\ln I(t\wedge\tau_M)}{t} \le \lim_{t\to\infty} \frac{\ln M}{t} = 0.$$

Since $N(s) \le M$ whenever $s \le \tau_M$, we have $0 \le N(t\wedge\tau_M) \le M$. Thus $\dfrac{N(t\wedge\tau_M)}{t} \le \dfrac{M}{t} \to 0$ as $t\to\infty$,
Taking $\liminf_{t\to\infty}$ of both sides of (59) gives, almost surely,

$$\beta\left(1+\frac{\gamma}{d}\right) \liminf_{t\to\infty} \bar{I}_{t,\,M} \ge c_0, \tag{60}$$

i.e.

$$\liminf_{t\to\infty} \bar{I}_{t,\,M} \ge \frac{c_0}{\beta(1+\gamma/d)} = \varepsilon^* > 0. \tag{61}$$

Finally, let $M\to\infty$. Since $\tau_M \uparrow \infty$ a.s. (Theorem 3.1), the stopped averages $\bar{I}_{t,\,M}$ and the unstopped average $\dfrac{1}{t}\int_0^t I(s)\,ds$ have the same lim inf a.s., yielding

$$\liminf_{t\to\infty} \frac{1}{t}\int_0^t I(s)\,ds \ge \varepsilon^* \quad \text{a.s.}$$

The bound in the above inequality gives persistence *in mean* through a time-averaged expectation. Although almost sure estimates are used to control the stochastic integrals in the proof, the conclusion itself concerns persistence in mean, not almost sure convergence of $I(t)$.

This completes the proof. □

7. Numerical simulation and discussion

In this section, we present numerical simulations to illustrate the theoretical results on extinction and persistence of the stochastic SIR model. The simulations are implemented using the Milstein scheme for stochastic differential equations, which provides strong convergence of order 1.0.

Numerical method (Milstein scheme) Consider the SDE system

$$\mathrm{d}S(t) = f_1(S,\, I,\, R)\,\mathrm{d}t + g_1(S,\, I,\, R)\,\mathrm{d}B_1(t),$$

$$\mathrm{d}I(t) = f_2(S,\, I,\, R)\,\mathrm{d}t + g_2(S,\, I,\, R)\,\mathrm{d}B_2(t),$$

$$\mathrm{d}R(t) = f_3(S,\, I,\, R)\,\mathrm{d}t + g_3(S,\, I,\, R)\,\mathrm{d}B_3(t),$$

with $g_i'(\cdot)$ denoting the derivative of g_i with respect to its state argument along the i-th component. The Milstein discretization with step Δt reads

$$S_{n+1} = S_n + f_1(S_n,\, I_n,\, R_n)\,\Delta t + g_1(S_n,\, I_n,\, R_n)\,\Delta B_1^n + \frac{1}{2}\,g_1(S_n,\, I_n,\, R_n)\,g_1'(S_n,\, I_n,\, R_n)\left[(\Delta B_1^n)^2 - \Delta t\right],$$

$$I_{n+1} = I_n + f_2(S_n,\, I_n,\, R_n)\,\Delta t + g_2(S_n,\, I_n,\, R_n)\,\Delta B_2^n + \frac{1}{2}\,g_2(S_n,\, I_n,\, R_n)\,g_2'(S_n,\, I_n,\, R_n)\left[(\Delta B_2^n)^2 - \Delta t\right],$$

$$R_{n+1} = R_n + f_3(S_n,\, I_n,\, R_n)\,\Delta t + g_3(S_n,\, I_n,\, R_n)\,\Delta B_3^n + \frac{1}{2}\,g_3(S_n,\, I_n,\, R_n)\,g_3'(S_n,\, I_n,\, R_n)\left[(\Delta B_3^n)^2 - \Delta t\right],$$

where $\Delta B_i^n \sim \mathcal{N}(0,\, \Delta t)$ are independent normal increments.

For the infection equation, the diffusion term is $g_2(I) = \sigma_2 I$, so its derivative is constant: $g_2'(I) = \sigma_2$. Therefore, the Milstein correction

$$\frac{1}{2}\,g_2(I_n)\,g_2'(I_n)\left[(\Delta B_2^n)^2 - \Delta t\right],$$

must be replaced explicitly by x

$$\frac{1}{2}\sigma_2^2 I_n\left[(\Delta B_2^n)^2 - \Delta t\right].$$

Hence, the explicit Milstein update for the infected population is

$$I_{n+1} = I_n + f_2(S_n,\, I_n,\, R_n)\,\Delta t + \sigma_2 I_n\,\Delta B_2^n + \frac{1}{2}\sigma_2^2 I_n\left[(\Delta B_2^n)^2 - \Delta t\right].$$

This term is required and was missing in the previously displayed scheme.

Unless noted otherwise, we use $\Delta t = 10^{-3}$ in the simulations.

The baseline parameters are chosen as $\Lambda = 5$, $\beta = 0.4$, $\gamma = 0.2$, and $d = 0.1$. Noise intensities $(\sigma_1,\, \sigma_2,\, \sigma_3)$ are varied to study both extinction and persistence regimes. Initial conditions are $(S_0,\, I_0,\, R_0) = (50,\, 10,\, 0)$.

Figure 1 depicts the deterministic SIR model in the absence of stochastic perturbations (i.e., $\sigma_1 = \sigma_2 = \sigma_3 = 0$). The curves show the time evolution of the susceptible (S), infected (I), and recovered (R) populations over a 600-day horizon. During the initial outbreak phase (0-50 days), the infection spreads rapidly because the susceptible pool is

large; correspondingly, $I(t)$ rises sharply as transmission dominates recovery and natural removal. Around the peak (roughly day ≈ 40), the infected population reaches its maximum, after which the depletion of susceptibles lowers the effective contact rate $\beta S(t)$ below the level needed for further growth. In the decline phase (50-150 days), $I(t)$ decreases approximately exponentially while $R(t)$ increases steadily, reflecting cumulative recoveries. For longer times ($t \gtrsim 150$ days). Deterministic SIR dynamics corresponding to the noise-free system. The trajectory converges to the endemic equilibrium

$$(S_o,\, I_o,\, R_o) = \left(\frac{d+\gamma}{\beta},\, \frac{\Lambda}{d} - \frac{d+\gamma}{\beta},\, \frac{\gamma}{d}\left(\frac{\Lambda}{d} - \frac{d+\gamma}{\beta}\right)\right),$$

which satisfies $I_o > 0$ only when

$$\tilde{R}_0 = \frac{\beta\,\Lambda}{d(d+\gamma)} > 1,$$

so the equilibrium shown is biologically feasible (endemic) precisely under the condition $\tilde{R}_0 > 1$. Overall, after brief transients, the trajectories become smooth and monotone toward the equilibrium, confirming that without stochastic effects, the dynamics converge to a stable mean-field endemic state.

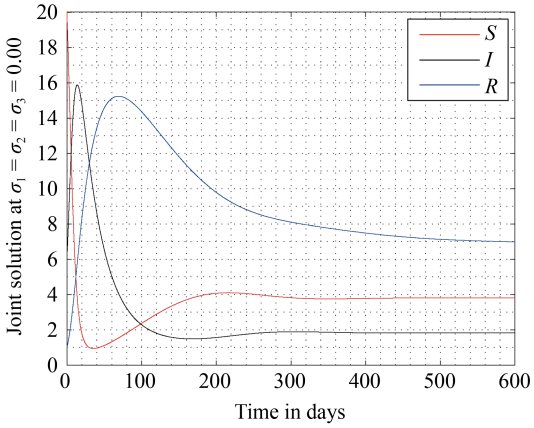

Figure 1. Deterministic trajectories of the SIR model with zero noise ($\sigma_1 = \sigma_2 = \sigma_3 = 0$)

Figure 2 illustrates the temporal evolution of the susceptible population $S(t)$ under increasing noise intensities $\sigma_1 = 0.02$, $\sigma_2 = 0.03$, and $\sigma_3 = 0.04$. In contrast to the smooth deterministic trajectory, the introduction of stochastic perturbations induces random oscillations around the mean equilibrium level. For small noise ($\sigma_1 = 0.02$), the susceptible curve exhibits mild fluctuations with short-term deviations but remains close to the deterministic path, indicating that the system's intrinsic stability is largely preserved. As the infection noise ($\sigma_2 = 0.03$) increases, the fluctuations become more pronounced, producing intermittent excursions both above and below the steady-state value; these correspond to random surges and declines in the number of susceptibles caused by environmental variability in the infection process. At higher stochastic intensity ($\sigma_3 = 0.04$), the amplitude of oscillations increases significantly, and the system displays irregular yet bounded behavior. This indicates that environmental noise amplifies the variability in $S(t)$ but does not destabilize the overall population balance. The results highlight that even moderate stochastic effects can create pronounced short-term variability around the deterministic equilibrium without changing the long-term mean trajectory.

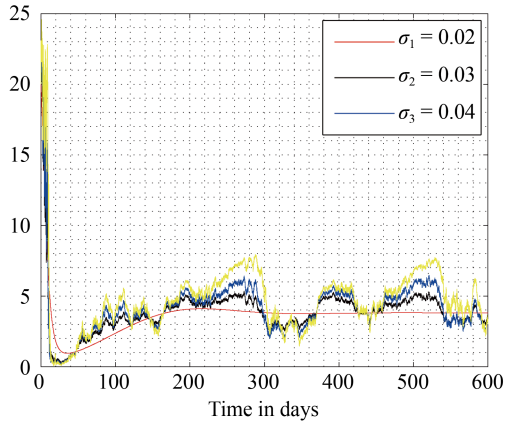

Figure 2. Stochastic trajectories of the susceptible population $S(t)$ for increasing noise intensities $\sigma_1 = 0.02$, $\sigma_2 = 0.03$, and $\sigma_3 = 0.04$

Figure 3 presents the temporal evolution of the infected population $I(t)$ under different noise intensities $\sigma_1 = 0.02$, $\sigma_2 = 0.03$, and $\sigma_3 = 0.04$. In all cases, the infection begins with a sharp outbreak as the initially large susceptible pool drives a rapid increase in new infections. However, after reaching the early peak near $t \approx 20$ days, the infected population decreases steadily due to recovery and the depletion of susceptibles. When $\sigma_1 = 0.02$, the trajectory remains relatively smooth, resembling the deterministic decay toward the endemic level. As the stochastic intensity increases ($\sigma_2 = 0.03$ and $\sigma_3 = 0.04$), random environmental fluctuations become more prominent, generating irregular oscillations and transient rebounds of $I(t)$ throughout the simulation period. These fluctuations reflect random perturbations in transmission and recovery rates, leading to short-lived epidemic resurgences. Despite the variability, the infection remains bounded, and the mean level of $I(t)$ stays low, indicating that stochasticity primarily modulates amplitude rather than causing instability. This behavior confirms that moderate noise intensities enhance the variability of epidemic outcomes while preserving the long-term stability of the infected population.

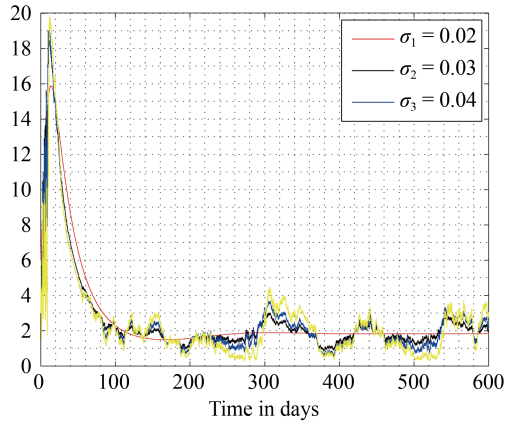

Figure 3. Stochastic trajectories of the infected population $I(t)$ for noise intensities $\sigma_1 = 0.02$, $\sigma_2 = 0.03$, and $\sigma_3 = 0.04$

Figure 4 illustrates the temporal dynamics of the recovered population $R(t)$ under varying noise intensities $\sigma_1 = 0.02$, $\sigma_2 = 0.03$, and $\sigma_3 = 0.04$. The recovered class exhibits a typical epidemic pattern: an initial rapid rise due to accumulated recoveries following the infection peak, followed by a gradual decline toward an equilibrium level as recovery and mortality balance the inflow of new infections. For low noise intensity ($\sigma_1 = 0.02$), the trajectory of $R(t)$ is smooth and closely follows the deterministic curve, displaying only minor deviations. As stochastic effects increase ($\sigma_2 = 0.03$ and

$\sigma_3 = 0.04$), noticeable fluctuations appear, corresponding to random surges and drops in the recovered population. These fluctuations arise from noise acting multiplicatively on the recovery process, producing variability in the rate at which individuals transition from the infected to the recovered class. Despite this irregularity, the general trend of convergence toward a bounded mean value remains evident. The system thus demonstrates robustness: stochastic perturbations amplify short-term variability but do not alter the long-term equilibrium behavior of $R(t)$. Overall, the results confirm that moderate environmental noise perturbs the recovery trajectory without destabilizing the global epidemic dynamics.

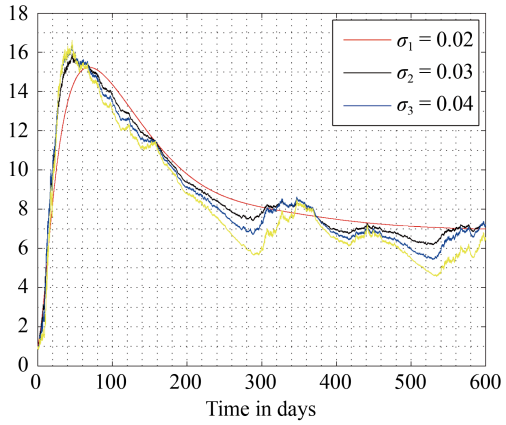

Figure 4. Temporal trajectories of the recovered population $R(t)$ under different noise intensities: $\sigma_1 = 0.02$, $\sigma_2 = 0.03$, and $\sigma_3 = 0.04$

8. Results and conclusion

Results summary. The analytical results demonstrate that the stochastic SIR model with multiplicative noise admits a unique, globally positive solution for all admissible initial conditions. By constructing appropriate Lyapunov functions, we established the extinction and persistence conditions in terms of the noise-adjusted basic reproduction number

$$\tilde{R}_0 = \frac{\beta(\Lambda/d)}{d+\gamma+\frac{1}{2}\sigma_2^2}.$$

When $\tilde{R}_0 < 1$, the infected population $I(t)$ tends to zero almost surely, and the system converges to the disease-free equilibrium $(S^*, I^*, R^*) = (\Lambda/d, 0, 0)$. Conversely, when $\tilde{R}_0 > 1$, the infection persists stochastically, fluctuating around a positive endemic level. The derived criteria extend the deterministic threshold $R_0 = \beta(\Lambda/d)/(d+\gamma)$ by accounting for the influence of environmental randomness through σ_2.

9. Numerical confirmation

Simulations conducted via the Milstein scheme confirm the theoretical predictions. For weak noise intensity, trajectories of $S(t)$, $I(t)$, and $R(t)$ closely follow their deterministic counterparts, exhibiting small-amplitude fluctuations around the endemic equilibrium. As the noise amplitude increases, stochastic effects generate irregular oscillations and short-term variability, yet the population processes remain bounded and biologically meaningful. At sufficiently large σ_2, the infection component decays to zero, validating the analytical extinction condition.

10. Biological interpretation

The results highlight the critical impact of environmental fluctuations on epidemic persistence. While deterministic models predict persistence whenever $R_0 > 1$, the stochastic formulation reveals that randomness in infection or recovery rates can suppress the disease even under favorable deterministic conditions. Hence, noise plays a stabilizing role by reducing the effective reproduction potential of the infection.

Authors' contributions

All authors contributed equally to conceptualization, analysis, and writing.

Acknowledgment

The author Mohammed Alghazi extends the appreciation to the Deanship of Postgraduate Studies and Scientific Research at Majmaah University for funding this research work through the project number (R-2025-2200).

Data availability

No datasets were generated or analyzed for this study.

Conflict of interest

The authors declare no competing financial interest.

References

[1] Kermack WO, McKendrick AG. A contribution to the mathematical theory of epidemics. *Proceedings of the Royal Society A*. 1927; 115(772): 700-721.

[2] Diekmann O, Heesterbeek JAP, Metz JAJ. On the definition and the computation of the basic reproduction ratio R_0 in models for infectious diseases in heterogeneous populations. *Journal of Mathematical Biology*. 1990; 28(4): 365-382.

[3] Anderson RM, May RM. *Infectious Diseases of Humans: Dynamics and Control*. Oxford: Oxford University Press; 1991.

[4] Chhetri B, Kumar BV. Stochastic mathematical modelling study for understanding the extinction, persistence and control of SARS-CoV-2 virus at the within-host level. *Hybrid*. 2025; 44: 372.

[5] Venkatesh A, Raj MP, Baranidharan B, Rahmani MKI, Tasneem KT, Khan M, et al. Analyzing steady-state equilibria and bifurcations in a time-delayed SIR epidemic model featuring Crowley-Martin incidence and Holling type II treatment rates. *Heliyon*. 2024; 10(21): e39520.

[6] Mahato P, Mahato SK, Das S. A stochastic epidemic model with Crowley-Martin incidence rate and Holling type III treatment. *Decision Analytics Journal*. 2024; 10: 100391.

[7] Hu X, Wang M, Dai X, Yu Y, Xiao A. A positivity preserving Milstein-type method for stochastic differential equations with positive solutions. *Journal of Computational and Applied Mathematics*. 2024; 449: 115963.

[8] Mohammad KM, Kamrujjaman M. Stochastic differential equations to model influenza transmission with continuous and discrete-time Markov chains. *Alexandria Engineering Journal*. 2025; 110: 329-345.

[9] Wu X, Yan Y. Milstein scheme for a stochastic semilinear subdiffusion equation driven by fractionally integrated multiplicative noise. *Fractal and Fractional*. 2025; 9(5): 314.

[10] Sabbar Y. A review of modern stochastic modeling: SDE/SPDE numerics, data-driven identification, and generative methods with applications in biology and epidemiology. *arXiv:2508.11004*. 2025. Available from: https://doi.org/10.48550/arXiv.2508.11004.
[11] Tornatore E, Buccellato SM, Vetro P. Stability of stochastic epidemic models with delays. *Physica A: Statistical Mechanics and Its Applications*. 2021; 565: 125580.
[12] Girardi P, Gaetan C. An SEIR model with time-varying coefficients for analyzing the SARS-CoV-2 epidemic. *Risk Analysis*. 2023; 43(1): 144-155.
[13] Ogunmiloro OM, Kareem H. Mathematical analysis of a generalized epidemic model with nonlinear incidence function. *Beni-Suef University Journal of Basic and Applied Sciences*. 2021; 10(1): 15.
[14] Li J. Analysis of a stochastic SIR model with media effects. *arXiv:2309.08126*. 2023. Available from: https://doi.org/10.48550/arXiv.2309.08126.
[15] Hussain S, Khan A, Baleanu D. A numerical and analytical study of a stochastic epidemic model under environmental white noise. *Computational and Mathematical Methods in Medicine*. 2022; 2022(1): 1638571.
[16] Rifhat R, Hattaf K, Yafia R. Extinction and persistence of a stochastic SIRV epidemic model with general nonlinear incidence. *Journal of Applied Mathematics*. 2021; 2021: 200.
[17] Yi X, Chen J, Li Y. Analysis of stochastic epidemic model with awareness: extinction and persistence. *Scientific Reports*. 2024; 14: 78218.
[18] Li S, Wang D, Zhang H. SIR epidemic model with general nonlinear incidence and Lévy jumps: existence, positivity and extinction. *Mathematics*. 2024; 12(2): 215.
[19] Ahmed R, Ali M, Khan S. Analysis and simulation of a stochastic SIR model with transmission perturbed by white noise. *Scientific Reports*. 2025; 15: 04142.
[20] Khan T, Ahmad S, Petkov P. Correlated stochastic epidemic model for the dynamics of SARS-CoV-2 with vaccination. *Scientific Reports*. 2022; 12: 20059.
[21] Alsakaji HJ, Abdelrahman M, Rihan FA. A stochastic epidemic model with time delays: existence, uniqueness and positivity of solutions. *Results in Control and Optimization*. 2024; 14: 100180.
[22] Settati A, Abid M, Rachik M. Stochastic SIR epidemic model dynamics on scale-free networks. *Physica A: Statistical Mechanics and Its Applications*. 2025; 642: 130434.
[23] Gasteratos I. *Moderate deviations for multiscale stochastic reaction-diffusion equations and related importance sampling schemes*. Doctoral Dissertation. Boston University; 2022.
[24] Wang L, Teng Z, Rifhat R, Wang K. Modelling of a drug resistant tuberculosis for the contribution of resistance and relapse in Xinjiang, China. *Discrete & Continuous Dynamical Systems-Series B*. 2023; 28(7): 4167-4189.
[25] ur Rahman G, Tymoshenko O, Di Nunno G. Insights on stochastic dynamics for transmission of monkeypox: biological and probabilistic behavior. *Mathematical Methods in the Applied Sciences*. 2025; 48(15): 14316-14333.
[26] Hussain S, Tunç O, ur Rahman G, Khan H, Nadia E. Mathematical analysis of stochastic epidemic model of MERS-corona & application of ergodic theory. *Mathematics and Computers in Simulation*. 2023; 207: 130-150.